Atmos. Chem. Phys., 11, 4085–4094, 2011
www.atmos-chem-phys.net/11/4085/2011/
doi:10.5194/acp-11-4085-2011

Atmospheric Chemistry and Physics

Impact of organic nitrates on urban ozone production

D. K. Farmer[1,*], A. E. Perring[1,], P. J. Wooldridge[1], D. R. Blake[4], A. Baker[4], S. Meinardi[4], L. G. Huey[5], D. Tanner[5], O. Vargas[5], and R. C. Cohen[1,2,3]**

[1]Department of Chemistry, University of California Berkeley, Berkeley, CA, 94720, USA
[2]Department of Earth and Planetary Science, University of California Berkeley, Berkeley, CA, 94720, USA
[3]Environmental Technologies Division, Lawrence Berkeley National Labs, Berkeley, CA, 94720, USA
[4]Department of Earth System Science, University of California Irvine, Irvine, CA, 92697, USA
[5]School of Earth and Atmospheric Sciences, Georgia Institute of Technology, Atlanta, GA, 30332, USA
[*]now at: Cooperative Institute for Research in Environmental Sciences and Department of Chemistry, University of Colorado, Boulder, CO, 80309, USA
[**]now at: Chemical Sciences Division, Earth System Research Laboratory, National Oceanic and Atmospheric Administration, Boulder, Colorado and Cooperative Institute for Research in Environmental Sciences, University of Colorado, Boulder, Colorado, USA

Received: 20 July 2010 – Published in Atmos. Chem. Phys. Discuss.: 11 October 2010
Revised: 8 February 2011 – Accepted: 26 April 2011 – Published: 4 May 2011

Abstract. Urban O_3 is produced by photochemical chain reactions that amplify background O_3 in mixtures of gaseous nitrogen oxides (NO_x) and organic molecules. Current thinking treats NO_x and organics as independent variables that limit O_3 production depending on the NO_x to organic ratio; in this paradigm, reducing organics either has no effect or reduces O_3. We describe a theoretical counterexample where NO_x and organics are strongly coupled and reducing organics increases O_3 production, and illustrate the example with observations from Mexico City. This effect arises from chain termination in the HO_x and NO_x cycles via organic nitrate production. We show that reductions in VOC reactivity that inadvertently reduce organic nitrate production rates will be counterproductive without concurrent reductions in NO_x or other organics.

1 Introduction

High concentrations of ozone (O_3) at the Earth's surface are widely recognized as unhealthy and are a target for public policies aimed at reducing occurrence of asthma and other cardiopulmonary diseases and at improving crop yields (Bell et al., 2005; Booker et al., 2009; Selin et al., 2009; Silverman et al., 2010). Production of surface O_3 is typically considered limited by either gas phase (volatile) organic molecules (VOC) or nitrogen oxides ($NO_x = NO + NO_2$), and control strategies to reduce O_3 typically target the limiting reagent. Here, we demonstrate that the production of organic nitrates (molecules of the form $RONO_2$) during oxidation of organics confounds the usual assumption that organics and NO_x are independent variables that can be considered separately in ozone control strategies, and show that in some cases organic reductions that are presumed in the standard conceptual model to be effective at reducing ozone can be counterproductive and result in ozone increases.

Tropospheric O_3 is produced by the catalytic oxidation of gas phase organic compounds in the presence of NO_x. Initiation of the catalysis begins with the production of radicals (most often OH) from either sunlight-driven photolysis or the reaction of O_3 with alkenes. OH reacts with VOC or CO, producing peroxy radicals (HO_2, RO_2). These peroxy radicals oxidize NO to NO_2, which is then photolyzed to produce the $O(^3P)$ atoms that react with O_2 to form O_3:

$$NO + HO_2 \rightarrow NO_2 + OH \quad \text{(R1)}$$

$$NO + RO_2 \rightarrow NO_2 + RO \quad \text{(R2a)}$$

$$NO_2 + h\nu \rightarrow NO + O(^3P) \quad \text{(R3)}$$

$$O(^3P) + O_2 \rightarrow O_3 \quad \text{(R4)}$$

In the presence of oxygen, the alkoxy radical (RO) produced in Reaction (R2a) typically isomerizes or decomposes,

Correspondence to: R. C. Cohen
(rccohen@berkeley.edu)

resulting in production of RO_2 or HO_2. Reaction of HO_2 with NO to reform OH completes the chain.

Ozone production (hereafter P_{O_3}) by this radical chain continues until termination. Most often, we consider the effects of two classes of termination reactions. First, in air with low NO_x to organic ratios (NO_x-limited regime), peroxide formation (R5) dominates chain termination:

$$RO_2 + HO_2 \rightarrow ROOH + O_2 \quad \text{(R5)}$$

In this regime, the addition of NO_x increases O_3 production by enhancing the rates of (R1) and (R2a), while addition of VOC has little effect on O_3 production rates as nearly every OH formed is already reacting with a VOC. In air with high NO_x to organic ratios (variously called VOC limited, NO_x saturated or NO_x suppressed), nitric acid (HNO_3) formation is the primary chain termination step:

$$OH + NO_2 \rightarrow HNO_3 \quad \text{(R6)}$$

In this regime, the addition of NO_x decreases O_3 production because NO_2 effectively competes with the available organics for OH. Ozone production rates increase when organics are added or when NO_x is removed. As a result of these competing chain termination reactions, P_{O_3} varies non-linearly with NO_x at constant VOC (Liu et al., 1988; Thornton et al., 2002; Murphy et al., 2007).

Chain termination can also occur in reactions that result from combining RO_2 and NO_x radicals to form either peroxy acyl nitrates (PNs = $RC(O)O_2NO_2$, Reaction R7) or alkyl and multifunctional nitrates (ANs = $RONO_2$, hereafter referred to as "alkyl nitrates", Reaction R2b):

$$RC(O)O_2 + NO_2 \leftrightarrow RC(O)O_2NO_2 \quad \text{(R7)}$$

$$NO + RO_2 \rightarrow RONO_2 \quad \text{(R2b)}$$

PNs are temporary reservoirs that release most of the NO_x soon (minutes to hours) after formation. On regional and global scales it is widely understood that PN formation redistributes NO_x, decreasing NO_x in the urban core and increasing NO_x downwind (Singh et al., 1981; Moxim et al., 1996; Heald et al., 2003; Hudman et al., 2004).

In contrast, ANs have been, with few exceptions (Shepson et al., 1993; Horowitz et al., 2007; Ito et al., 2009; Perring et al., 2009), considered nearly permanent sinks for NO_x with consequences that are only local. Specific effects of AN formation on global- and continental-scale O_3 in response to climate change have been the focus of recent model studies (Wu et al., 2007; Ito et al., 2009; Weaver et al., 2009). However, little attention has been paid to effects of AN formation on urban O_3 and thus O_3 control strategies. This is true both for simplified analytical models which often neglect the reactions leading to AN formation and for computationally intensive chemical transport models which represent chemistry using lumped mechanistic elements that reduce computing demands but do not accurately represent AN production.

The main goal of this paper is to analyze a simplified model of atmospheric chemistry, thus providing intuition about interpreting the combined effects of VOC reactivity and alkyl nitrate branching ratios in more complex chemical transport models representing urban air pollution and investigating possible control strategies. We also show that the hypothetical scenarios we discuss have relevance to thinking about a real world situation using analysis of observations from Mexico City.

2 Methods and measurements

2.1 Site

Measurements were made at the T1 site at the Universidad Tecnical de Tecámac (UTTEC) in Tecámac, MX (19.703° N latitude, 98.982° W longitude, 2273 m elevation) as part of the MILAGRO (Megacity Impacts on Local, Global and Regional Environments) campaign. Inlets and instruments were located on the university campus, which is ∼30 km to the north of Mexico City, and lies between a large, unmanaged field and a large road that was a few hundred meters uphill and to the north of the site, typically downwind during the daytime. The site was located such that prevailing winds should be a few hours downwind from downtown Mexico City. Inlets for $NO_{y,i}$ species (NO_2, ΣPNs, $\Sigma ANs_{(gas+aerosol)}$, and $HNO3_{(gas+aerosol)}$), O_3, and CO were co-located approximately 10 m above ground level; instruments were kept in temperature-controlled containers. Measurements described in this paper were taken between 17 March and 29 March 2006.The site was characterized by mid-afternoon average temperature highs of 25 °C and pre-sunrise lows of 10 °C. Thunderstorms and precipitation were observed on several late-afternoons. The boundary layer grew rapidly in the mid-morning to 2–3 km (Fast et al., 2007).

2.2 Instrumentation

NO_2, ΣPNs, $\Sigma ANs_{(gas+aerosol)}$, and $HNO3_{(gas+aerosol)}$ were measured by the UC Berkeley thermal dissociation-laser induced fluorescence (TD-LIF) detector (Day et al., 2002). Briefly, air is pulled through a heated PFA inlet into a resistively-heated quartz tube, or oven. Classes of NO_{yi} species are thermally dissociated to NO_2 and an accompanying radical at temperatures characteristic of their bond energies. For example, in the configuration used during the MILAGRO campaign, peroxy and peroxy acyl nitrates (ΣPNs, $\Sigma R_iO_2NO_2$) dissociate to NO_2 and RO_2 radicals at 180 °C, alkyl and multifunctional nitrates (ΣANs, ΣR_iONO_2) dissociate to NO_2 and RO radicals by 360 °C, and HNO_3 dissociates to NO_2 and OH at 620 °C. The difference in NO_2 detected in adjacent channels is thus the sum of each class: the ΣPNs mixing ratio is the difference in NO_2 signal detected in a 180 °C oven and NO_2 detected in an unheated oven. HONO

is not detected in this system and N_2O_5 dissociates in the ΣPNs channel. Semi-volatile particle-phase organic nitrates are expected to dissociate in the ΣANs channel, and semi-volatile particulate HNO_3 (i.e., NH_4NO_3) dissociates in the HNO_3 channels with unit efficiency (Rollins et al., 2010). During these experiments, a glass pinhole was placed at the entrance to the inlet to create a large pressure drop before air entered the ovens. This pressure drop minimized the effects of secondary chemistry on the observed concentrations. As a result, corrections that have been required at high NO or high O_3 for other inlet configurations were unnecessary.

NO_2 is detected by laser-induced fluorescence by exciting ground-state NO_2 radicals at 408 nm with a littrow configuration tunable diode laser (Toptica DL100). Laser power was at 9mW for the duration of the campaign, and the linewidth is <1 MHz. Measurements were taken at 1 Hz, averaged to three minutes and interpolated to a common time basis.

The TD-LIF was maintained in a 2 oven-2 cell mode in which NO_2 signal is detected from pairs of oven temperatures in two cells for approximately 25 min before the oven temperatures were ramped to the next pair of temperatures. For example, the two ovens would be set at 180 °C and 360 °C to measure ΣANs, and then cooled to ambient and 180 °C to measure NO_2 and ΣPNs. Oven temperatures were overlapped during the ramping cycles at least once a day to intercompare and confirm that ovens set at identical temperatures detected identical NO_2. The duty cycle to directly measure the full suite of NO_{yi} classes was 100 min. Note that ΣPNs and NO_2 were simultaneously measured for 50 min of each ramp cycle. For this analysis, data were interpolated to obtain a simultaneous set of NO_{yi} measurements. Comparison of the ΣPN and ΣAN measurements using TD-LIF shows they have accuracy comparable to independent methods (Perring et al., 2010; Wooldridge et al., 2010).

O_3 was measured by a commercial UV photometric O_3 analyzer (TECO Model 49C). CO was measured by a modified commercial non-dispersed IR adsorption instrument (Thermo Environmental Systems, Model 48C) (Parrish et al., 1994). NO was measured by a chemiluminescence detector (Ryerson et al., 2000). VOCs were measured by Proton-Transfer Ion Trap Mass Spectrometry (Warneke et al., 2005), in situ gas chromatography, and ex situ GC analysis from canister samples.

2.3 Data analysis

We calculated observed VOC reactivity (s^{-1}) as the sum of VOC mixing ratios, including CH_4, scaled by their OH reactivity:

$$\tau_{VOC} = \sum_i k_{OH+VOC_i}[VOC_i] \quad (1)$$

Total OH reactivity was calculated by including CO, NO_x, HNO_3, SO_2, O_3, peroxides and peroxy radicals.

Rosen et al. (2004) described in detail how the observed branching ratio is calculated from the ratio of O_x (O_3 + NO_2) versus alkyl nitrates. Briefly, the instantaneous production rates of alkyl nitrates and O_3 ($P_{\Sigma ANs}$ and P_{O_3}, respectively) can be described by

$$P_{\Sigma ANs} = \sum_i \alpha_i k_{OH+VOC_i}[OH][VOC_i] \quad (2)$$

$$P_{O_3} = \sum_i \gamma_i (1-\alpha_i) k_{OH+VOC_i}[OH][VOC_i] \quad (3)$$

where, for an individual VOC_i, α_i is the branching ratio and γ_i the number of O_3 produced, typically 2 (Rosen et al., 2004). Assuming that the VOC mixture is dominated by species with $\gamma_i = 2$ and that the effective branching ratio of the entire VOC mix (α) is relatively small ($\ll$1), α can be related to the ratio of O_3 to ΣAN production (Rosen et al., 2004). If near enough to the VOC source to ignore deposition and entrainment, the ratio of O_3 to ΣAN production can be approximated by observed changes (Δ) in O_x and ΣANs:

$$\frac{\Delta O_x}{\Delta \Sigma ANs} \approx \frac{P_{O_3}}{P_{\Sigma ANs}} \approx \frac{2(1-\alpha)}{\alpha} \approx \frac{2}{\alpha} \quad (4)$$

Using this relationship, we determined the effective branching ratio for the field site from observed O_3, NO_2 and ΣANs. Note that this calculation assumes that all ANs observed by the TD-LIF are formed in the gas-phase through Reaction (R2b), whether they were observed in the gas or particle phase.

We calculate the VOC precursors of the observed ΣANs following Rosen et al. (2004). The relative contribution of each VOC to an instantaneous ΣAN production was calculated from the VOC reactivity of the individual species ($\tau_{VOC,i}$) scaled by the species' branching ratio (α_i) and rate constant with respect to NO (k_{NO+RO_2}), normalized by the total production rate calculated as the sum over all ΣAN production (Eq. 5):

$$\frac{P_{AN,i}}{P_{\Sigma ANs}} = \frac{\tau_{VOC,i} k_{NO+RO_2} \alpha_i}{\sum_i \tau_{VOC,i} k_{NO+RO_2} \alpha_i} \quad (5)$$

We use average afternoon (12:00 p.m.–06:00 p.m.) concentrations of each observed species to represent VOC reactivity. Several VOC species likely to be contributors to alkyl nitrate formation were not measured; to account for these, expected average afternoon mixing ratios were estimated from mixing ratios and relative abundance observed in the Mexico City region during the MCMA 2003 campaign (Dunlea et al., 2007) (starred entries in Table S1). These compounds represent <15 % of the total OH reactivity. Mixing ratios, branching ratios and rate constants used in this analysis are summarized in Table S1. This analysis includes observed ΣANs as precursors, which are expected to react with OH radicals to become further functionalized (Rosen et al., 2004) and possibly form di-nitrates.

2.4 Observations

Daytime total OH reactivity ranged from 3–34 s^{-1}, with NO_2 comprising 9–35 % of the total during the day, and VOC and CO ranging 43–69 % of the total. The contributions to the afternoon reactivity were due to CO (31 %), CH_4 (7 %), saturated hydrocarbons (13 %), unsaturated hydrocarbons (29 %), ΣANs (5 %), and C_6–C_{11} aromatics (7 %), with aldehydes, ketones, alcohols, and formaldehyde making up the remaining 8 %. Aromatic concentrations largely follow the diurnal cycle of VOC reactivity but they contribute a larger fraction of VOC reactivity in the evening and morning than at midday (12 % vs. 7 %) indicating that they are a larger fraction of primary emissions. While benzene and toluene each comprise a third of observed nocturnal aromatics, they account for almost all (benzene 56 %, toluene 43 %) aromatic concentrations at peak O_3 (02:00 p.m.). Daily ΣAN maxima were observed at noon and O_3 maxima were observed at ~02:00 p.m. ΣANs were correlated with O_x (= O_3 + NO_2), consistent with previous observations in urban and rural environments (Day et al., 2003; Rosen et al., 2004; Cleary et al., 2005) and with our analysis of export in the Mexico city plume (Perring et al., 2010).

Relative contributions of VOC classes to OH reactivity and ΣAN production are shown in Fig. S1. As AN branching ratios for aromatics are less well established than for some of the other categories, the contribution of aromatics to ANs is calculated with two different estimated yields to provide an upper and lower limit of their contribution. The lower branching ratios are described in the table (5 % for benzene and toluene, 10 % for xylene, 8 % for all other aromatics), and are used throughout the paper unless otherwise specified. The upper estimates for aromatic branching ratios are 5 % for benzene and toluene, 10 % for xylene and 25 % for all other aromatics.

3 Discussion

3.1 Analysis

The effects of AN chemistry on P_{O_3} can be represented by a quadratic equation (Eqs. 6–12) that describes the coupled kinetics of Reactions (R1–R7) (Murphy et al., 2006). The equation describes P_{O_3} at a single time of day, and is derived from the understanding that HO_x (= OH + HO_2 + RO_2) radicals are in steady state. Using this equation is a reasonable approximation to the effects that would be observed in a fully coupled chemical transport model as peak P_{O_3} occurs at noon and is strongly correlated with observed O_3 maxima. As HO_x is assumed to be in steady-state, the production and loss rates are equal:

$$P_{HO_x} = L_{HO_x} = k_{OH+NO_2} \times [OH][NO_2] + \alpha \times k_{NO+RO_2} \times [NO][RO_2] + 2k_{HO_2+HO_2} \times [HO_2][HO_2] + 2k_{RO_2+HO_2} \times [HO_2][RO_2] + 2k_{RO_2+RO_2} \times [RO_2][RO_2] \quad (6)$$

As described by Murphy et al. (2006), under conditions of rapid ozone production in which chain propagation dominates, every RO_2 produced via VOC oxidation by OH reacts with an NO radical (Reaction R2) and results in an HO_2 radical following reaction of the alkoxy radical with O_2. Thus, HO_x can be expressed as:

$$[HO_2] \approx [RO_2] \approx \frac{\tau_{VOC}[OH]}{(1-\alpha)k_{NO+RO_2}[NO]} \quad (7)$$

Following Murphy et al. (2006), the instantaneous P_{O_3} is approximated from Eq. (3):

$$P_{O_3} = k_{HO_2+NO}[HO_2][NO] + k_{RO_2+NO}[RO_2][NO] = 2 \times \tau_{VOC} \times [OH_{calc}] \quad (8)$$

Combining the above equations and solving for OH, one finds:

$$OH_{calc} = \frac{-b \pm \sqrt{b^2 - 4ac}}{2a} \quad (9)$$

where

$$a = \left(2k_{HO_2+HO_2} + 2k_{RO_2+HO_2} + 2k_{RO_2+RO_2}\right) \times \left(\frac{\tau_{VOC}}{(1-\alpha) \times k_{NO+RO_2} \times [NO]}\right)^2 \quad (10)$$

$$b = k_{OH+NO_2} \times [NO_2] + \frac{\alpha \times k_{NO+RO_2} \times \tau_{VOC}}{(1-\alpha)k_{NO+RO_2}} \quad (11)$$

$$c = -P_{HO_x} \quad (12)$$

In the above equations, τ_{VOC} is the VOC reactivity to OH (s^{-1}), α is the effective AN branching ratio for the ambient mix of VOC and P_{HO_x} is the HO_x production rate. Rate constants for HO_2 self-reaction ($k_{HO_2+HO_2}$), HO_2-RO_2 reactions ($k_{HO_2+RO_2}$) and RO_2 self-reaction ($k_{RO_2+RO_2}$) were taken from the 15th JPL evaluation (Sander et al., 2006) and are 2.74×10^{-12}, 8×10^{-12} and 6.8×10^{-14} cm^3 $molec^{-1}$ s^{-1}, respectively. These numbers assume that rates for $C_2H_5O_2$ are exemplary of all RO_2, as described in Perring et al. (2001).

3.2 Theoretical examples

Figure 1a–d shows calculations of P_{O_3} using this equation with $P_{HO_x} = 3.5 \times 10^6$ molec cm^{-3} s^{-1} and $\alpha = 0$, 0.035, 0.07 and 0.13. An increase in α causes a decrease in P_{O3} independent of VOC reactivity. At larger VOC reactivity the effect is slightly larger. For example, doubling α from 3.5 % to 7 % with a VOC reactivity of 5 s^{-1} causes a 21 % decrease in peak P_{O_3}, but the same change in α at a VOC reactivity of 10 s^{-1}causes a 26 % decrease in P_{O_3}. The effect of α on maximum P_{O_3} can be approximated as (1-α)$^{2\times \text{chain length}}$, where chain length is the ratio of propagation to initiation rates for O_3 formation through the steps described above. This is useful to keep in mind as it helps to explain why $RONO_2$ production is not important at high NO_x where chain lengths

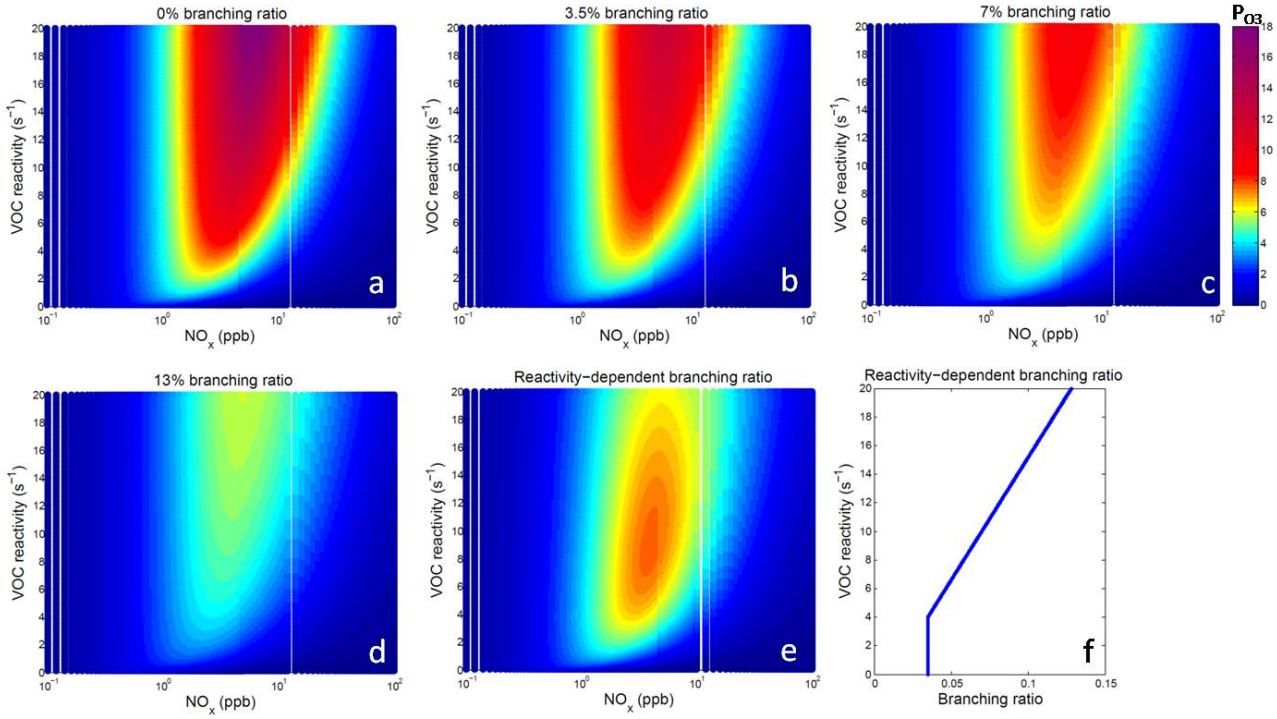

Fig. 1. Ozone production (P_{O_3}, ppb h^{-1}) derived from an analytic model is plotted as a function of NO_x and VOC reactivity under four different organic nitrate scenarios with branching ratios of 0 % **(a)**, 3.5 % **(b)**, 7 % **(c)**, 13 % **(d)** and a VOC-dependant branching ratio **(e)**. Given a single organic nitrate branching ratio **(a–d)**, increasing VOCs increases P_{O_3}; in the NO_x-limited regime, increasing NO_x increases P_{O_3} until a maximum is reached and the system becomes VOC-limited. Ignoring organic nitrate production severely over-estimates P_{O_3} maxima **(a)** compared to the 7 % AN branching ratios scenario **(b)** observed in Mexico City. A scenario in which VOC decreases are accompanied by a reduction in branching ratio from 13 to 3.5 % between VOC reactivities of 20 and 4 s^{-1} **(f)** demonstrates the case in which the P_{O_3} maximum is centered **(e)**. Decreasing VOC reactivity may actually increase P_{O_3}, counter to current thinking.

are only 1 or 2. AN formation also affects the NO_x concentration at which the system transitions from NO_x-limited to VOC-limited by a policy relevant percentage. For a given reactivity, maximum P_{O_3} occurs at a higher NO_x when the calculation uses lower branching ratios. For example, at a reactivity of 4.5 s^{-1}, ignoring AN formation ($\alpha = 0$ %), we find peak P_{O_3} at 3.0 ppb NO_x; with a 7 % branching ratio peak P_{O_3} occurs at 2.8 ppb NO_x. This shift of peak-NO_x increases with reactivity: the same branching ratio shift ($\alpha = 0$ % to 7 %) at a higher reactivity of 9 s^{-1} results in a 13 % change in the NO_x where P_{O_3} peaks.

The strong suppression of P_{O_3} by AN formation shown in Fig. 1a–d implies that organic emission reductions that affect the branching ratios in Reaction (R2) will affect P_{O_3}. For example, we have observed higher average branching rations in urban environs ($\alpha = 5$–10 %) than in rural ones ($\alpha = 3$–4 %) (Rosen et al., 2004; Perring et al., 2009, 2010). If we assume reducing VOC emissions results in a transition from an urban to rural VOC mix, then the reduction in α will lead to an increase in O_3 production. Note that branching ratios for isoprene range from 4 % to 12 % (Tuazon et al., 1990; Chen et al., 1998; Sprengnether et al., 2002; Patchen et al., 2007; Paulot et al., 2009; Perring et al., 2009), and that depending on the choice of urban mix and effective biogenic branching ratio, the effect on P_{O_3} would vary. To illustrate the effect we are describing, Fig. 1e shows a calculation of P_{O_3} for α decreasing from 0.13 to 0.035 as reactivity decreases from 20 s^{-1} to 4 s^{-1} (Fig. 1f). The figure demonstrates that accounting for the effects of $RONO_2$ formation can fundamentally change the shape of the P_{O_3} contour map with a peak occurring in the center rather than the nearly vertical ridge line shown in Fig. 1a–d. Although there are a number of other metrics for considering the effects of VOC changes on P_{O_3} (e.g. incremental reactivity, ozone production potential, Pickering et al., 1990; FinlaysonPitts et al., 1997), to our knowledge none of these methods has a functional form capable of predicting an increase in ozone in response to VOC reductions.

This figure uses a larger branching ratio than we have observed in the atmosphere to exaggerate the effect we are describing. A more realistic scenario is useful to indicate how $RONO_2$ chemistry would effect a policy relevant discussion of VOC vs. NO_x reductions. For the purposes of evaluating policy options, it is common to consider examples where

VOC or NO_x emissions are reduced by about 30 %. Using that as a metric, in Fig. 2 we compare the effect of two hypothetical ozone reduction strategies to a reference case with 7 % branching ratio and $\tau_{VOC} = 4.5\,s^{-1}$ (the solid P_{O_3} curve in Fig. 2). In the first strategy we imagine uniform emission reductions that result in a 30 % reduction in organic reactivity with no change to α (the lowest, dashed P_{O_3} curve in Fig. 2). The result is a decrease in P_{O_3} for $NO_x > 0.7$ ppb; this decrease changes with NO_x mixing ratios, approaching 20 % above 5 ppb NO_x. If instead the same 30 % reduction of VOC reactivity occurs concurrently with a decrease in α from 7 % to 3.5 % (the dotted curve in Fig. 2) the result is mixed. At high NO_x where HNO_3 formation dominates chain termination, VOC controls are effective. In this example, VOC controls do not reduce P_{O_3} by at least 10 % unless NO_x is over 8 ppb. However, peak ozone production rates increase and ozone production increases at all values of NO_x below 3 ppb, making it likely that ozone will increase at all locations downwind of the urban core. As a result of these calculations, we believe that much more careful attention to the effect of $RONO_2$ formation on P_{O_3} will provide new insights into optimal urban O_3 control strategies. We note that these calculations consider a single NO:NO_2 ratio, and that the assumptions required for Eq. (7) may not hold for the low-NO_x/high VOC reactivity regime of the upper left corner of Fig. 1a–e. For example, for a VOC reactivity of $5\,s^{-1}$, the assumption that every RO_2 reacts with NO is invalid at NO concentrations on the order of a ppt, as reactions with HO_2 radicals become significant. At higher VOC reactivities, the break-down of the assumption occurs at higher NO_x concentrations: for example, for an airmass with $20\,s^{-1}$ VOC reactivity, the assumption required for Eq. (7) breaks down at 0.4 ppb NO. Additionally, HO_2 and RO_2 radicals can react with O_3,

$$HO_2 + O_3 \rightarrow OH + 2O_2 \quad \text{(R8)}$$

$$RO_2 + O_3 \rightarrow RO + 2O_2 \quad \text{(R9)}$$

Reaction (R8) produces OH radicals, thus effectively recycling HO_x radicals. For 60 ppb O_3, this reaction accounts for >5 % of the HO_2 sinks when NO_x is <0.2 ppb and HO_2 is high. In parallel to HO_2, $RO_2 + O_3$ reactions effectively recycle $RO_2 + HO_2$ radicals, and have no significant effect on the modeled HO_x and P_{O_3}. The reaction rate for Reaction (R9) is approximately 200 times slower than Reaction (R8) (Tyndall et al., 1998), and cannot compete with other RO_2 reactions in our model system. While the NO:NO_2 ratio depends on O_3, HO_2 and RO_2, and thus varies, the algebraic solution presented is accurate for an instantaneous choice of those variables, and the values used in this manuscript are typical of observations made in Mexico City.

3.3 Application to Mexico City

To illustrate with an example, this chemistry is likely important to the options for ozone control in Mexico City. O_3 production in the Mexico City area is in a NO_x-suppressed regime (Lei et al., 2007; Tie et al., 2007). This is most evident in increased odd-oxygen levels on weekends in response to the decreased NO_x concentrations (Stephens et al., 2008). Long-term studies show that NO_x and CO decreased over the last 20 yr by 10 and 70 %, respectively (Arriaga-Colina et al., 2004; Stephens et al., 2008). Total VOC concentrations have been essentially constant (Arriaga-Colina et al., 2004). PAN concentrations have decreased from daily maxima of 34 to 15 ppb between 1997 and 2003. This is a steeper decrease than in NO_x and is likely due to reduced emissions of specific hydrocarbons (Marley et al., 2007).

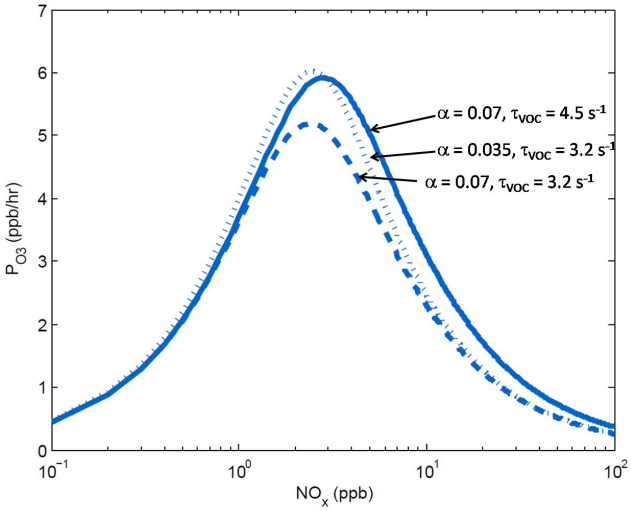

Fig. 2. Under three sample VOC-NO_x regimes, P_{O_3} varies as a function of NO_x: for observed conditions in Mexico City (solid line; VOC reactivity of $4.5\,s^{-1}$, ANs branching ratio of 7 %); a 30 % reduction in VOC reactivity with no change in branching ratio (dashed line, $3.2\,s^{-1}$, 7 %), and a combined 30 % reduction in VOC reactivity and subsequent 3.5 % branching ratio, the result of targeted reduction in aromatics and other high-branching ratio VOCs (dotted line).

As described in Sect. 2.3, we use the slope of the $O_x - \Sigma$ANs correlation (Fig. 3) to derive an effective branching ratio α of 7±1 % (1σ). Observations of C_1-C_4 ANs show they account for 5–10 % of the observed ΣANs. We estimate fractional contributions of observed organics to the total ΣANs, finding that 5 % of alkyl nitrates are derived from oxidation of C_1 to C_4 alkanes, 10–26 % are derived from aromatic VOCs, and 29–35 % are derived from unsaturated hydrocarbons (Fig. S1). Longer-chain saturated hydrocarbons are 24–29 % of the AN precursors and ΣANs themselves 8–10 %. The predicted branching ratio is 4 %, about half of what we observe, indicating that there are additional high AN yield compounds that were not measured; the predicted branching ratio is similar to the difference between AN yields inferred from the O_3-ΣAN correlation and observed VOC in other urban areas including Sacramento and Houston (Rosen

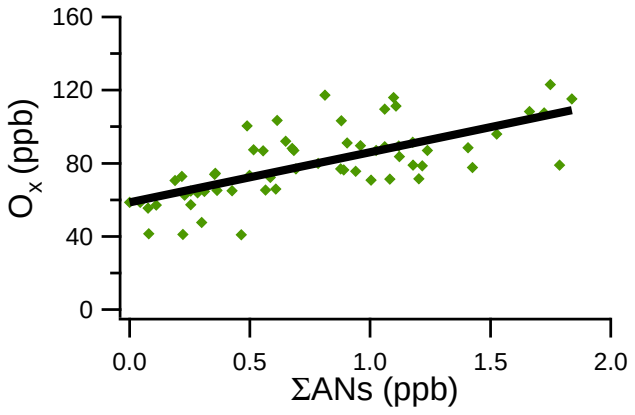

Fig. 3. The net branching ratio of 7 % for total alkyl nitrates in the Mexico City region is calculated from the slope (27 ppb ppb^{-1}) of the correlation of O_x ($NO_2 + O_3$) and ΣANs observations.

et al., 2004; Cleary et al., 2005). These results from the Tecamac ground site are consistent with concurrent aircraft observations taken in and downwind of the Mexico City plume (Perring et al., 2010).

As the effective α is so high (larger than we have observed in other cities), it is reasonable to imagine that control strategies targeting O_3 or particulate matter would alter the effective branching ratio of the hydrocarbon mixture in Mexico City. This could occur as a transition to a rural mixture dominated by lower-α_i VOCs as described in the theoretical example above, or by direct management of anthropogenic emissions. For example, long chain hydrocarbons are thought to be important to secondary organic aerosol (SOA) and might be deliberately reduced in an attempt to lower SOA. These chemicals also have some of the largest branching ratios (∼30 %) to AN formation (Lim et al., 2009). We calculate that an emission control strategy resulting in a selective 50 % reduction of the C_5 and larger alkanes that we measured would reduce VOC reactivity by 4 % and α by 14 %. Starting with the reference case in Fig. 2 (4.5 s^{-1}, $\alpha = 7$ %), this change would increase peak P_{O_3} from 5.9 ppb h^{-1} to 6.1 ppb h^{-1}. Note that if the AN branching ratio effect on P_{O_3} described in this paper is ignored (i.e., $\alpha = 0$), a 4 % reduction in VOC reactivity from 4.5 s^{-1} reduces peak P_{O_3} in this model from 8.4 to 8.2 ppb h^{-1}. It is now believed that a class of intermediate volatility organic compounds (IVOC) are not measured by current techniques but react rapidly to form SOA in urban plumes (Robinson et al., 2007). These IVOC would have high (∼30 %) AN yields. If we assume they are an additional 4 % of the reactivity, removal of these molecules would increase P_{O_3} by 6 % to 6.3 ppb h^{-1}. Similarly, AN formation from aromatics are estimated to occur more efficiently than the average VOC (Atkinson et al., 2003; Wagner et al., 2003). Aromatics have been dramatically reduced in the US through use of reformulated fuels and one might imagine a similar control strategy could be implemented in Mexico City. However, the branching ratios for aromatics are poorly known for the first oxidation stage and completely unknown for subsequent oxidation steps. As described above (Sect. 2.4), we calculate aromatic ANs yields with both low and high branching ratios. The higher values are intended to represent the possible range for chemical production of ANs in subsequent stages of aromatic oxidation. Aromatic precursors contribute 10 % of ΣANs for the lower yields and 26 % for higher yields. The higher yields raise the effective branching ratio by 17–19 %, depending on whether potential IVOC are included in the calculation. Complete removal of aromatics would either result in no change in the P_{O_3} maximum (5.9 ppb h^{-1}, low aromatic branching ratios) or increase the P_{O_3} maximum by 3 % to 6.1 ppb h^{-1} (high aromatic branching ratios). If instead of complete removal we imagine 50 % removal of C_5 and larger alkanes, IVOC and aromatics, we predict that peak P_{O_3} would increase by 5–6 %. These effects are magnified for systems with higher VOC reactivity: for a system with twice the VOC reactivity (9 s^{-1}), a 50 % removal of C_5 and larger alkanes, IVOC and aromatics would result in an 8–9 % increase in the P_{O_3} maximum. It should be noted that the history of air quality control measures has focused on reducing vapor pressure – an action which had the likely consequence of increasing α, while current trends toward replacing gasoline with higher vapor pressure fuels (e.g. ethanol) act in the converse to decrease α.

Perring et al. (2010) demonstrated that the ΣAN branching ratio can decrease with photochemical age as an urban plume evolves, changing from 12 % to 2 % with 50 h of processing. This is consistent with ground-based observations that branching ratios in urban areas are typically higher than in rural areas, suggesting that the concurrent effect of changing VOC mix and ΣAN branching ratios on P_{O_3} is relevant over a wide range of atmospherically relevant regimes (Perring et al., 2010).

4 Conclusions

AN formation, a relatively minor reaction that is more or less ignored in the standard models guiding air pollution control strategies, is surprisingly important. We show both in a model and with a real world example of Mexico City that the effects of AN formation can counteract the benefits of VOC reductions on ozone production. Under circumstances of significant photochemistry and high VOC reactivity, removing VOCs can change the effective ΣAN branching ratio, potentially increasing O_3 production and changing the NO_x and VOC dependence of P_{O_3}. This chemistry may also be a partial explanation for why ozone reductions are slowing in Los Angeles, a city where VOC controls have until recently been effective. Independent of these two examples, the effect of AN production on O_3 formation rates indicates that additional thought should be given to AN formation in

designing air quality control strategies and additional attention should be given to understanding the chemical mechanisms for production of ANs and to accurately representing them in the photochemical mechanisms used for air quality modeling. At present, chemical mechanisms used in urban and regional air quality models do not treat AN formation in detail in the first stage of oxidation, let alone in the subsequent ones. The problem may be even more severe for multifunctional oxidation products for which there are relatively few constraints from the laboratory. Until the mechanisms in such models are evaluated, approximate calculations could be used to supplement those models in planning.

Supplementary material related to this article is available online at: http://www.atmos-chem-phys.net/11/4085/2011/acp-11-4085-2011-supplement.pdf.

Acknowledgements. The authors thank Joost de Gouw from NOAA-ESRL for additional VOC data. This research was funded by NSF grants ATM-0639847 and ATM-0511829.

Edited by: I. Trebs

References

Arriaga-Colina, J. L., West, J. J., Sosa, G., Escalona, S. S., Ordunez, R. M., and Cervantes, A. D. M.: Measurements of VOCs in Mexico City (1992-2001) and evaluation of VOCs and CO in the emissions inventory, Atmos. Environ., 38, 2523–2533, 2004.

Atkinson, R. and Arey, J.: Gas-phase tropospheric chemistry of biogenic volatile organic compounds: a review, Atmos. Environ., 37, S197–S219, 2003.

Bell, M. L., Dominici, F., and Samet, J. M.: A meta-analysis of time-series studies of ozone and mortality with comparison to the national morbidity, mortality, and air pollution study, Epidemiology, 16, 436–445, 2005.

Booker, F., Muntifering, R., McGrath, M., Burkey, K., Decoteau, D., Fiscus, E., Manning, W., Krupa, S., Chappelka, A., and Grantz, D.: The Ozone Component of Global Change: Potential Effects on Agricultural and Horticultural Plant Yield, Product Quality and Interactions with Invasive Species, J. Int. Plant Biol., 51, 337–351, 2009.

Chen, X. H., Hulbert, D., and Shepson, P. B.: Measurement of the organic nitrate yield from OH reaction with isoprene, J. Geophys. Res., 103, 25563–25568, 1998.

Cleary, P. A., Murphy, J. G., Wooldridge, P. J., Day, D. A., Millet, D. B., McKay, M., Goldstein, A. H., and Cohen, R. C.: Observations of total alkyl nitrates within the Sacramento Urban Plume, Atmos. Chem. Phys. Discuss., 5, 4801–4843, doi:10.5194/acpd-5-4801-2005, 2005.

Day, D. A., Wooldridge, P. J., Dillon, M. B., Thornton, J. A., and Cohen, R. C.: A thermal dissociation laser-induced fluorescence instrument for in situ detection of NO_2, peroxy nitrates, alkyl nitrates, and HNO_3, J. Geophys. Res., 107, 4046, doi:10.1029/2001JD000779, 2002.

Day, D. A., Dillon, M. B., Wooldridge, P. J., Thornton, J. A., Rosen, R. S., Wood, E. C., and Cohen, R. C.: On alkyl nitrates, O_3, and the "missing NO_y", J. Geophys. Res., 108, 4501, doi:10.1029/2003JD003685, 2003.

Dunlea, E. J., Herndon, S. C., Nelson, D. D., Volkamer, R. M., San Martini, F., Sheehy, P. M., Zahniser, M. S., Shorter, J. H., Wormhoudt, J. C., Lamb, B. K., Allwine, E. J., Gaffney, J. S., Marley, N. A., Grutter, M., Marquez, C., Blanco, S., Cardenas, B., Retama, A., Ramos Villegas, C. R., Kolb, C. E., Molina, L. T., and Molina, M. J.: Evaluation of nitrogen dioxide chemiluminescence monitors in a polluted urban environment, Atmos. Chem. Phys., 7, 2691–2704, doi:10.5194/acp-7-2691-2007, 2007.

Fast, J. D., de Foy, B., Acevedo Rosas, F., Caetano, E., Carmichael, G., Emmons, L., McKenna, D., Mena, M., Skamarock, W., Tie, X., Coulter, R. L., Barnard, J. C., Wiedinmyer, C., and Madronich, S.: A meteorological overview of the MILAGRO field campaigns, Atmos. Chem. Phys., 7, 2233–2257, doi:10.5194/acp-7-2233-2007, 2007.

FinlaysonPitts, B. J. and Pitts, J. N.: Tropospheric air pollution: Ozone, airborne toxics, polycyclic aromatic hydrocarbons, and particles, Science, 276, 1045–1052, 1997.

Heald, C. L., Jacob, D. J., Fiore, A. M., Emmons, L. K., Gille, J. C., Deeter, M. N., Warner, J., Edwards, D. P., Crawford, J. H., Hamlin, A. J., Sachse, G. W., Browell, E. V., Avery, M. A., Vay, S. A., Westberg, D. J., Blake, D. R., Singh, H. B., Sandholm, S. T., Talbot, R. W., and Fuelberg, H. E.: Asian outflow and trans-Pacific transport of carbon monoxide and ozone pollution: An integrated satellite, aircraft, and model perspective, J. Geophys. Res., 108, 4804, doi:10.1029/2003JD003507, 2003.

Horowitz, L. W., Fiore, A. M., Milly, G. P., Cohen, R. C., Perring, A., Wooldridge, P. J., Hess, P. G., Emmons, L. K., and Lamarque, J. F.: Observational constraints on the chemistry of isoprene nitrates over the eastern United States, J. Geophys. Res., 112, D12S08, doi:10.1029/2006JD007747, 2007.

Hudman, R. C., Jacob, D. J., Cooper, O. R., Evans, M. J., Heald, C. L., Park, R. J., Fehsenfeld, F., Flocke, F., Holloway, J., Hubler, G., Kita, K., Koike, M., Kondo, Y., Neuman, A., Nowak, J., Oltmans, S., Parrish, D., Roberts, J. M., and Ryerson, T.: Ozone production in transpacific Asian pollution plumes and implications for ozone air quality in California, J. Geophys. Res., 109, D23S10, doi:10.1029/2004JD004974, 2004.

Ito, A., Sillman, S. and Penner, J. E.: Global chemical transport model study of ozone response to changes in chemical kinetics and biogenic volatile organic compounds emissions due to increasing temperatures: Sensitivities to isoprene nitrate chemistry and grid resolution, J. Geophys. Res., 114, D09301, doi:10.1029/2008JD011254, 2009.

Lei, W., de Foy, B., Zavala, M., Volkamer, R., and Molina, L. T.: Characterizing ozone production in the Mexico City Metropolitan Area: a case study using a chemical transport model, Atmos. Chem. Phys., 7, 1347–1366, doi:10.5194/acp-7-1347-2007, 2007.

Lim, Y. B. and Ziemann, P. J.: Effects of Molecular Structure on Aerosol Yields from OH Radical-Initiated Reactions of Linear, Branched, and Cyclic Alkanes in the Presence of NO_x, Environ. Sci. Technol., 43, 2328–2334, 2009.

Liu, S. C. and Trainer, M.: Responses of the Tropospheric Ozone and Odd Hydrogen Radicals to Column Ozone Change, J. Atmos. Chem., 6, 221–233, 1988.

Marley, N. A., Gaffney, J. S., Ramos-Villegas, R., and Cárdenas González, B.: Comparison of measurements of peroxyacyl nitrates and primary carbonaceous aerosol concentrations in Mexico City determined in 1997 and 2003, Atmos. Chem. Phys., 7, 2277–2285, doi:10.5194/acp-7-2277-2007, 2007.

Moxim, W. J., Levy, H., and Kasibhatla, P. S.: Simulated global tropospheric PAN: Its transport and impact on NO_x, J. Geophys. Res., 101, 12621–12638, 1996.

Murphy, J. G., Day, D. A., Cleary, P. A., Wooldridge, P. J., Millet, D. B., Goldstein, A. H., and Cohen, R. C.: The weekend effect within and downwind of Sacramento: Part 2. Observational evidence for chemical and dynamical contributions, Atmos. Chem. Phys. Discuss., 6, 11971–12019, doi:10.5194/acpd-6-11971-2006, 2006.

Murphy, J. G., Day, D. A., Cleary, P. A., Wooldridge, P. J., Millet, D. B., Goldstein, A. H., and Cohen, R. C.: The weekend effect within and downwind of Sacramento – Part 1: Observations of ozone, nitrogen oxides, and VOC reactivity, Atmos. Chem. Phys., 7, 5327–5339, doi:10.5194/acp-7-5327-2007, 2007.

Parrish, D. D., Holloway, J. S., and Fehsenfeld, F. C.: Routine, Continuous Measurement of Carbon-Monoxide with Parts-Per-Billion Precision, Environ. Sci. Technol., 28, 1615–1618, 1994.

Patchen, A. K., Pennino, M. J., Kiep, A. C., and Elrod, M. J.: Direct kinetics study of the product-forming channels of the reaction of isoprene-derived hydroxyperoxy radicals with NO, Int. J. Chem. Kinet., 39, 353–361, 2007.

Paulot, F., Crounse, J. D., Kjaergaard, H. G., Kroll, J. H., Seinfeld, J. H., and Wennberg, P. O.: Isoprene photooxidation: new insights into the production of acids and organic nitrates, Atmos. Chem. Phys., 9, 1479–1501, doi:10.5194/acp-9-1479-2009, 2009.

Perring, A. E., Bertram, T. H., Wooldridge, P. J., Fried, A., Heikes, B. G., Dibb, J., Crounse, J. D., Wennberg, P. O., Blake, N. J., Blake, D. R., Brune, W. H., Singh, H. B., and Cohen, R. C.: Airborne observations of total $RONO_2$: new constraints on the yield and lifetime of isoprene nitrates, Atmos. Chem. Phys., 9, 1451–1463, doi:10.5194/acp-9-1451-2009, 2009.

Perring, A. E., Bertram, T. H., Farmer, D. K., Wooldridge, P. J., Dibb, J., Blake, N. J., Blake, D. R., Singh, H. B., Fuelberg, H., Diskin, G., Sachse, G., and Cohen, R. C.: The production and persistence of $\Sigma RONO_2$ in the Mexico City plume, Atmos. Chem. Phys., 10, 7215–7229, doi:10.5194/acp-10-7215-2010, 2010.

Pickering, K. E., Thompson, A. M., Dickerson, R. R., Luke, W. T., McNamara, D. P., Greenberge, J. P., and Zimmerman, P. R.: Model calculations of tropospheric ozone production potential following observed convective events, J. Geophys. Res., 95, 14049–14062, 1990.

Robinson, A. L., Donahue, N. M., Shrivastava, M. K., Weitkamp, E. A., Sage, A. M., Grieshop, A. P., Lane, T. E., Pierce, J. R., and Pandis, S. N.: Rethinking organic aerosols: Semivolatile emissions and photochemical aging, Science, 315, 1259–1262, 2007.

Rollins, A. W., Smith, J. D., Wilson, K. R., and Cohen, R. C.: Real Time In Situ Detection of Organic Nitrates in Atmospheric Aerosols, Environ. Sci. Technol., 44, 5540–5545, 2010.

Rosen, R. S., Wood, E. C., Wooldridge, P. J., Thornton, J. A., Day, D. A., Kuster, W., Williams, E. J., Jobson, B. T., and Cohen, R. C.: Observations of total alkyl nitrates during Texas Air Quality Study 2000: Implications for O_3 and alkyl nitrate photochemistry, J. Geophys. Res., 109, D07303, doi:10.1029/2003JD004227, 2004.

Ryerson, T. B., Williams, E. J., and Fehsenfeld, F. C.: An efficient photolysis system for fast-response NO_2 measurements, J. Geophys. Res., 105, 26447–26461, 2000.

Sander, S. P., Finlayson-Pitts, B. J., Friedl, R. R., Golden, D. M., Huie, R. E., Keller-Rudek, H., Kolb, C. E., Kurylo, M. J., Molina, M. J., Moortgat, G. K., Orkin, V. L., Ravishankara, A. R., and Wine, P. H.: Chemical kinetics and photochemical data for use in atmospheric studies, Evaluation Number 15 in JPL Publication 06-2, Jet Propulsion Laboratory, 2006.

Selin, N. E., Wu, S., Nam, K. M., Reilly, J. M., Paltsev, S., Prinn, R. G., and Webster, M. D.: Global health and economic impacts of future ozone pollution, Environ. Res. Lett., 4, 044014, doi:10.1088/1748-9326/4/4/044014, 2009.

Shepson, P. B., Anlauf, K. G., Bottenheim, J. W., Wiebe, H. A., Gao, N., Muthuramu, K., and Mackay, G. I.: Alkyl Nitrates and Their Contribution to Reactive Nitrogen at a Rural Site in Ontario (Vol 27a, Pg 749, 1993), Atmos. Environ., 27, 2251–2251, 1993.

Silverman, R. A. and Ito, K.: Age-related association of fine particles and ozone with severe acute asthma in New York City, Journal of Allergy and Clinical Immunology, 125, 367–373, 2010.

Singh, H. B. and Hanst, P. L.: Peroxyacetyl Nitrate (Pan) in the Unpolluted Atmosphere – an Important Reservoir for Nitrogen-Oxides, Geophys. Res. Lett., 8, 941–944, 1981.

Sprengnether, M., Demerjian, K. L., Donahue, N. M., and Anderson, J. G.: Product analysis of the OH oxidation of isoprene and 1,3-butadiene in the presence of NO, J. Geophys. Res., 107, 4268, doi:10.1029/2001JD000716, 2002.

Stephens, S., Madronich, S., Wu, F., Olson, J. B., Ramos, R., Retama, A., and Muñoz, R.: Weekly patterns of México City's surface concentrations of CO, NO_x, PM_{10} and O_3 during 1986–2007, Atmos. Chem. Phys., 8, 5313–5325, doi:10.5194/acp-8-5313-2008, 2008.

Thornton, J. A., Wooldridge, P. J., Cohen, R. C., Martinez, M., Harder, H., Brune, W. H., Williams, E. J., Roberts, J. M., Fehsenfeld, F. C., Hall, S. R., Shetter, R. E., Wert, B. P., and Fried, A.: Ozone production rates as a function of NO_x abundances and HO_x production rates in the Nashville urban plume, J. Geophys. Res., 107, 4146, doi:10.1029/2001JD000932, 2002.

Tie, X. X., Madronich, S., Li, G. H., Ying, Z. M., Zhang, R. Y., Garcia, A. R., Lee-Taylor, J., and Liu, Y. B.: Characterizations of chemical oxidants in Mexico City: A regional chemical dynamical model (WRF-Chem) study, Atmos. Environ., 41, 1989–2008, 2007.

Tuazon, E. C. and Atkinson, R.: A Product Study of the Gas-Phase Reaction of Isoprene with the Oh Radical in the Presence of NO_x, Int. J. Chem. Kinet., 22, 1221–1236, 1990.

Tyndall, G. S., Wallington, T. J., and Ball, J. C.: FTIR product study of the reactions CH3O2+CH3O2 and CH_3O_2+O-3, J. Phys. Chem. A, 102, 2547–2554, 1998.

Wagner, V., Jenkin, M. E., Saunders, S. M., Stanton, J., Wirtz, K, and Pilling, M. J.: Modelling of the photooxidation of toluene: conceptual ideas for validating detailed mechanisms, Atmos. Chem. Phys., 3, 89–106, doi:10.5194/acp-3-89-2003, 2003.

Warneke, C., de Gouw, J. A., Lovejoy, E. R., Murphy, P. C., Kuster, W. C., and Fall, R.: Development of proton-transfer ion trap-mass spectrometry: On-line detection and identification of volatile organic compounds in air, J. Am. Soc. Mass Spectrom.,

16, 1316–1324, 2005.

Weaver, C. P., Liang, X. Z., Zhu, J., Adams, P. J., Amar, P., Avise, J., Caughey, M., Chen, J., Cohen, R. C., Cooter, E., Dawson, J. P., Gilliam, R., Gilliland, A., Goldstein, A. H., Grambsch, A., Grano, D., Guenther, A., Gustafson, W. I., Harley, R. A., He, S., Hemming, B., Hogrefe, C., Huang, H. C., Hunt, S. W., Jacob, D. J., Kinney, P. L., Kunkel, K., Lamarque, J. F., Lamb, B., Larkin, N. K., Leung, L. R., Liao, K. J., Lin, J. T., Lynn, B. H., Manomaiphiboon, K., Mass, C., McKenzie, D., Mickley, L. J., O'Neill, S. M., Nolte, C., Pandis, S. N., Racherla, P. N., Rosenzweig, C., Russell, A. G., Salathe, E., Steiner, A. L., Tagaris, E., Tao, Z., Tonse, S., Wiedinmyer, C., Williams, A., Winner, D. A., Woo, J. H., Wu, S., and Wuebbles, D. J.: A Preliminary Synthesis of Modeled Climate Change Impacts on Us Regional Ozone Concentrations, B. Am. Meteorol. Soc., 90, 1843–1863, 2009.

Wooldridge, P. J., Perring, A. E., Bertram, T. H., Flocke, F. M., Roberts, J. M., Singh, H. B., Huey, L. G., Thornton, J. A., Wolfe, G. M., Murphy, J. G., Fry, J. L., Rollins, A. W., LaFranchi, B. W., and Cohen, R. C.: Total Peroxy Nitrates (ΣPNs) in the atmosphere: the Thermal Dissociation-Laser Induced Fluorescence (TD-LIF) technique and comparisons to speciated PAN measurements, Atmos. Meas. Tech., 3, 593–607, doi:10.5194/amt-3-593-2010, 2010.

Wu, S. L., Mickley, L. J., Jacob, D. J., Logan, J. A., Yantosca R. M., and Rind, D.: Why are there large differences between models in global budgets of tropospheric ozone?, J. Geophys. Res., 112, D05302, doi:10.1029/2006JD007801, 2007.